POSMEC 2016 – Postgraduate Symposium in Mechanical Engineering
Department of Mechanical Engineering – Federal University of Uberlandia
December, 1st to 2nd, Uberlandia, Minas Gerais, Brazil

FORMATION OF FRICTION WELDING JOINTS IN NICKEL SUPERALLOYS

Igor Ziakhor, E.O. Paton Electric Welding Institute, zyakhor@paton.kiev.ua
Myroslav Zavertannyi, E.O. Paton Electric Welding Institute, zavrtannyi@gmail.com
Maksym Ziberov, Federal University of Uberlandia, ziberov@hotmail.com

Abstract: *Peculiarities of friction welding of nickel alloy EI698VD (Waspalloy analogue) are considered. Mathematical calculations made on the basis of the developed mathematical model of FW show that an alloy EI698VD can reach its melting temperature within the contact zone during the heating process. Experimental data are given on evaluation of microstructure of the alloy EI698VD welded joints. The results of the optical microscopy and scanning electron microscopy of welded joints using JEOL Field Emission Auger Microprobe JAMP-9500F are presented. Sound joints containing no microcracks can be provided through optimizing parameters of friction welding.*

Keywords*: friction welding, nickel alloy, mathematical model, melting temperature, welded joints.*

1. INTRODUCTION

Friction welding (FW) is used to advantage to manufacture nickel superalloys components of aircraft engines operating at high temperatures and under high loads. It is a known fact that for the sound joints to be formed in FW, it is necessary to generate a certain deformation, which would provide displacement of oxides and adsorbed films outside the sections of workpieces (Friction Welding, 2006). The deformation temperature range (DTR) of a superalloy depends upon its chemical composition, mechanical properties, and phase characteristics - solvus temperature $T_{\gamma'}$ (complete dissolution of the strengthening γ′-phase), and solidus temperature Ts. To evaluate phase changes in metal (degree of degradation of the γ′-phase) within the welded joint zone, it is necessary to know the data on temperature-time conditions of formation of joints on specific alloys. As direct measurements of the temperature of metal within the contact zone in FW are difficult, it is of a research and practical interest to calculate thermal cycles of FW of some superalloys.

Wrought nickel alloy EI698VD (alloy Waspalloy analogue) is used to manufacture components of gas turbine engines. The purpose of this study was to calculate thermal cycles of FW of alloy EI698VD depending upon the welding process parameters, to evaluate thermal-deformation conditions of formation of welded joints microstructure.

2. EXPERIMENTAL PROCEDURE

Experiments on FW were conducted on samples of the alloy EI698VD with a diameter of 16.0 mm. Nominal chemical composition of the alloy are given in Tab. (1). Main phase characteristics and DTR of alloy EI698VD are as follow: $T_{\gamma'}$ =1020 ºC, T_S=1320 ºC. Experiments were carried out by using FW machine ST120 (Zyakhor, 2001). The technology was developed for hybrid friction welding with controlled deformation (Kuchuk-Yatsenko e Zyakhor, 2004). Values of process parameters were varied within the following ranges: heating pressure P_h = 100-500 MPa, forging pressure P_F = 200-600 MPa, circumferential velocity V = 0.5-2.0 m/s, heating time t_h = 3-15 s, and forging time t_F = 5 s.

Table 1: Nominal chemical composition of alloy EI698VD.

Content of elements, %										
Ni	C	Cr	Ti	Al	Nb	Mo	Fe	B	Mn	Ce
Bal	0.03-0.07	13.00-16.00	2.35-2.75	1.45-1.80	1.90-2.20	2.80-3.20	≤2.00	0.05	≤0.40	0.005

Microstructure of the welded joints was examined by optical microscope “Neophot-32. Microstructure of the joints was revealed by electrolytic, chemical and ion etching using the JEOL Ion Sputter JFC-1100. The morphology of γ′-phase in the alloy EI698VD joining zone was investigated by JEOL Field Emission Auger Microprobe JAMP-9500F equipped with the “Oxford Instruments” EDS-analyser INCA-450. Microhardness of the joining zone metal was measured by LECO M400 hardness tester.

3. TEMPERATURE-TIME CONDITIONS OF FORMATION OF WELDED JOINTS

The data on temperature fields were generated by using the developed mathematical model of the heating process occurring in friction welding. The calculations were based on using the transient thermal conductivity equation and characteristics of consumption of power by a material during the FW process. The data on temperature fields were generated by using the developed mathematical model of the heating process occurring in FW. The calculations were based on using the transient thermal conductivity equation and characteristics of consumption of power by a material during the FW process.

Temperature field T (r, z, t) at arbitrary moment T is determined from known temperature field T (r, z, t - Δt) = T at moment t - Δt, where r- distance along radius of samples, z - distance along rotation axis of samples, Δt is the time step in tracing variations in the temperature field, starting from the initial state at t = 0. Temperature T = T (r, z, t) at each tracing step was determined by the variational method through minimising the next functional Eq. (1).

$$Э_T = -\frac{1}{2}\iint_S \left[r\lambda\left(\frac{\partial T}{\partial r}\right)^2 + r\lambda\left(\frac{\partial T}{\partial z}\right)^2 + rc\gamma\frac{T^2}{\Delta t} - \right.$$
$$\left. - 2rT\left(\frac{T_*}{\Delta t}c\gamma + W\right)\right] drdz + \frac{1}{2}\int_\Gamma r\alpha_T\left(T - 2T_c\right)Td\Gamma, \quad (1)$$

where $\lambda = \lambda(T)$ is the coefficient of thermal conductivity of a material; $c\gamma = c\gamma(T)$ is the volumetric heat capacity; W = W (r, z, t) is the heat source related to friction; S is the cross section area of a workpiece in plane (r, z); Γ is the profile confining surface S, on which a boundary condition is set for heat exchange with the environment, following the Newton's law, at heat exchange coefficient α_T; and T_c is the temperature of the environment.

Minimizing functional Eq. (1) according to T (r, z, t) yields a two-dimensional thermal conductivity equation in the cylindrical system of coordinates r and z (Eq. (2)).

$$\frac{\partial}{\partial r}\left(\lambda r\frac{\partial T}{\partial r}\right) + r\frac{\partial}{\partial z}\left(\lambda\frac{\partial T}{\partial z}\right) + W\cdot r = rc\gamma\frac{\partial T}{\partial t} - 2\alpha_T\left(T_c - T\right) \quad (2)$$

The initial temperature was assumed equal to 20 ºC, and boundary conditions corresponded to the conditions of heat exchange with the environment (Eq. (3)).

$$\lambda\frac{\partial T}{\partial r} = -\alpha_T\left(T_c - T\right),\ \lambda\frac{\partial T}{\partial z} = -\alpha_T\left(T_c - T\right)\cdot \quad (3)$$

Power of the heat source, W (r, z, t), was determined from the following formula (Eq. (4)).

$$W = P\cdot v_r\cdot F_r, \quad (4)$$

where P is the friction pressure, v_r is the circumferential velocity; and F_r is the friction coefficient of the mating surfaces.

The value of Fr in FW of alloy EI698VD was determined experimentally. Heat was generated over the entire friction surface, allowing for the fact that in formation of the liquid phase in the joining zone, no heat was generated in this location, and liquid metal was expelled into flash. The temperature problem was solved by the finite element method. Functional Eq. (1) corresponds to a quadratic form, which is a sum of all the elements in the region under consideration (Eq. (5)).

$$Э_н = -\frac{1}{2}\sum_m\sum_n\left\{(r\lambda)_{m,n}\left[\left(\frac{T_{m,n} - T_{m-1,n}}{\Delta r_{m,m-1}}\right)^2 + \right.\right.$$
$$\left.\left. + \left(\frac{T_{m,n} - T_{m,n-1}}{\Delta z_{n,n-1}}\right)^2\right] - 2W_{m,n}T_{m,n}r_{m,n}\right\}\Delta r_{m,m-1}\Delta z_{n,n-1}. \quad (5)$$

Minimizing quadratic form Eq. (5) by the values of temperature $T_{m,n}$ in the right top node of a finite element yields the following system of algebraic linear Eq. (6).

$$T_{m+1,n}\lambda_{m+1,n}r_{m+1}\frac{\Delta z_{n+1,n}}{\Delta r_{m+1,m}}+T_{m,n+1}\lambda_{n,n+1}r_m\frac{\Delta r_{m,m+1}}{\Delta z_{n+1,n}}+$$
$$+T_{m-1,n}\lambda_{m,n}r_m\frac{\Delta z_{n,n-1}}{\Delta r_{m,m-1}}+T_{m,n-1}\lambda_{m,n}r_m\frac{\Delta r_{m,m-1}}{\Delta z_{n,n-1}}-$$
$$-T_{m,n}\left[r_m\lambda_{m,n}\frac{\Delta z_{n,n-1}}{\Delta r_{m,m-1}}+r_{m+1}\lambda_{m+1,n}\frac{\Delta z_{n,n+1}}{\Delta r_{m+1,n}}+\right. \tag{6}$$
$$\left.+r_m\lambda_{m,n+1}\frac{\Delta r_{m,m-1}}{\Delta z_{n+1,n}}+\frac{c\gamma_{m,n}}{\Delta t}r_m\Delta r_{m,m-1}\Delta z_{n,n-1}\right]+$$
$$+\left(W_{m,n}+\frac{c\gamma_{m,n}}{\Delta t}T_{m,n}^{(k-1)}\right)r_m\Delta r_{m,m-1}\Delta z_{n,n-1}=0;$$

(m = 1, 2, ..., M; n = 1, 2, ..., N),

where M is the quantity of finite elements along radius r, and N is the quantity of elements along rotation axis z.

To complete the statement of the problem, it is necessary to add the following boundary conditions to the system of Eq. (6) is shown in Eq. (6a) and Eq. (6b).

$$\lambda\frac{T_{m,n}-T_{m-1,n}}{\Delta r_{m,m-1}}=-\alpha_T\left(T_c-T_{m,n}\right), \tag{6a}$$

$$\lambda\frac{T_{m,n}-T_{m-1,n}}{\Delta z_{n,n-1}}=-\alpha_T\left(T_c-T_{m,n}\right). \tag{6b}$$

The system of Eq. (6, 6a and 6b) was solved by the Gaussian method. The process thermal cycles were calculated for FW of the 16 mm diameter solid bars of alloy EI698VD, allowing for its thermal-physical properties (Tab. (2)). The results obtained on the distribution of temperature in samples at V_r= 2.0 m/s and V_r= 1.0 m/s are shown in Fig. (1).

Table 2: Thermal-physical properties of alloy EI698VD.

T, ºC	50	100	200	300	400	500	600	700	800	900	1000	1100	1200
$c\gamma \times 10^3$, J/(m^3·ºC)	3.76	3.80	3.88	4.00	4.15	4.33	4.54	4.96	5.50	5.50	5.42	5.38	5.38
λ, W/(m·ºC)	11.7	11.7	13.4	14.6	15.9	17.6	19.7	21.3	23.0	24.7	24.7	24.7	24.7

Calculation of distribution of temperature T (x, t) after a short period of friction time, i.e. 0.5-3.5 s, showed exceeding the solidus temperature of alloy EI698VD. At a substantial temperature gradient in axial and radial directions, no expelling of metal from the joint occurs in the contact zone at this stage of the process. Oscillograms of variations in the upsetting value, taken at different welding parameters, show that axial shortening (upsetting) of samples begins in about 2.0 s. A layer of the liquid phase, ΔX, was excluded from the calculations after this period of time, as it was expelled into a flash, and the temperature field moved to the friction surface on its both sides, tending to the ΔX value.

Therefore, as shown by the calculations, the temperature during a short period of time amounts to the values, at which some molten regions can be formed within the zone of contact of metals being joined. As the values of the friction torque and power of heat generation remain at a high level in all the phases of the welding process, it is likely that the melt is formed in separate regions of the peripheral part of contact surface, which further on are subjected to intensive deformation, move in a radial direction, and are pressed out from the joint into a flash.

Analysis of the calculations results shows that the increase in pressure leads to increase in heat generation in the contact zone. Intensification of heating with increase in pressure is compensated for by increase in the upsetting speed, which is accompanied by expelling the heated metal from the joint.

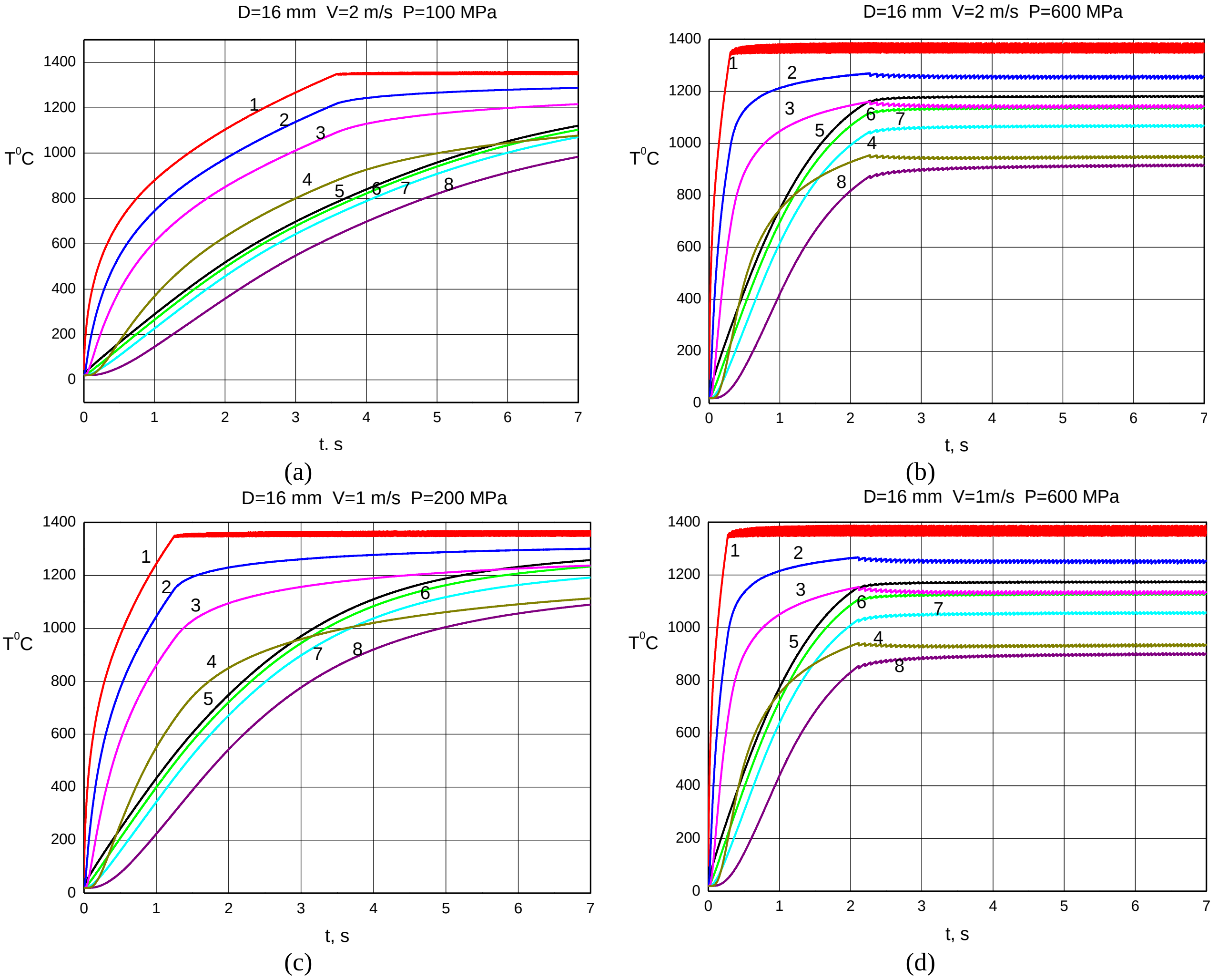

Figure 1: Variations in temperature of 16 mm diameter solid pieces of alloy EI698VD in FW at different distances from contact surface z (axial direction) and centre of section r (radial direction) at V_r = 2 (a, b) and 1 m/s (c, d), P_h = 100 (a), 200 (c) and 600 MPa (b, d): 1 – z = 0, r = 8 mm; 2 – z = 0.5 mm, r = 8 mm; 3 – z = 1 mm, r = 8 mm; 4 – z = 2 mm, r = 8 mm; 5 – z = 0, r = 0; 6 – z = 0.5 mm, r = 0; 7 – z = 1 mm, r = 0; 8 – z = 2 mm, r = 0.

The temperature gradient grows along z (rotation axis) with increase in pressure at all the values of the circumferential velocity. The distribution of temperature along z after FW at heating time t_h= 8 s for different values of P_h is shown in Fig. (2).

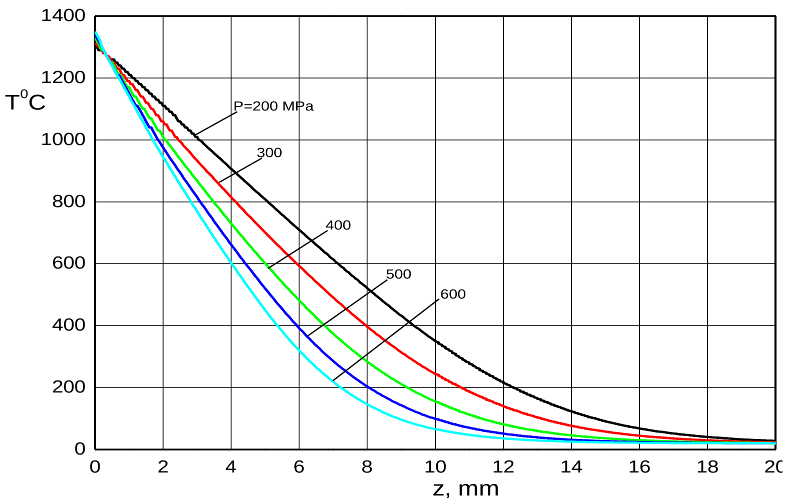

Figure 2: Temperature fields in joining zone on alloy EI698VD after FW at V_r =1.0 m/s.

The calculation results show that, as the solidus temperature is achieved in the contact zone during the heating process, one might expect dissolution of the strengthening γ′-phase in the joining zone at any values of the process parameters. Here the width of the phase transformation zone is determined by the temperature field, namely by width of the heat affected zone (HAZ) that was heated to a temperature above $T_{\gamma'}$. As seen from Fig. (1) and Fig. (2) the width of HAZ decreases with decreases in V_r and increase in P_h. As shown by the calculations, to minimize unfavourable phase transformations within the narrow joining zone in FW it is necessary to apply comparatively low values of the circumferential velocity and high values of pressure.

The calculated thermal cycles are confirmed by the data of microhardness analysis and metallographic examinations of welded joints on alloy EI698VD produced by changing the FW process parameters over wide ranges. The character of microhardness distribution of metal within the joining zone (JZ) and is similar at different FW process parameters, the difference being in width of the softening zone (Fig. (3)).

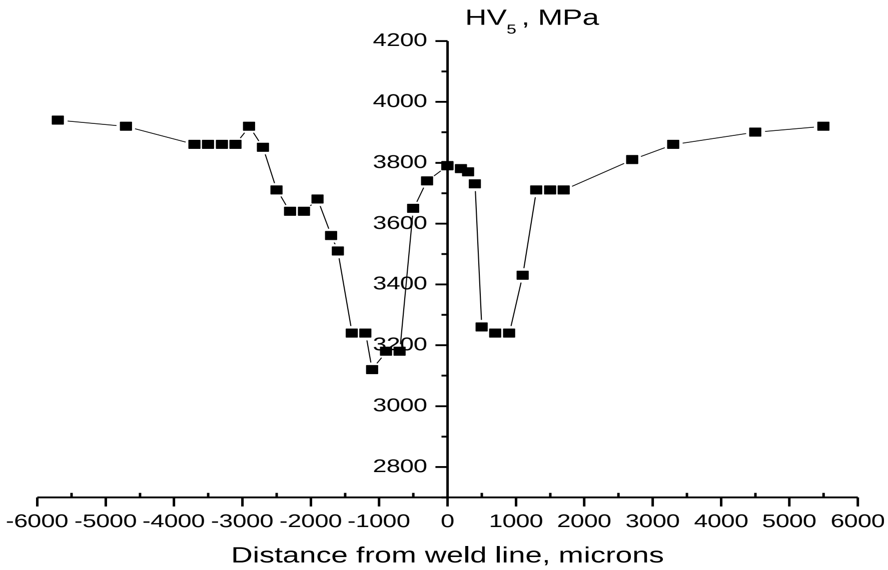

Figure 3: Microhardness distribution in FW joints on alloy EI698VD.

Increase in microhardness of metal at the center of the joint is related to substantial grain refinement (Fig. (4)), this being caused by the process of dynamic recrystallization of metal of this zone. The absence of the cast structure of metal in the JZ and HAZ is indicative of the absence of the risk of hot cracking in FW of alloy EI698VD.

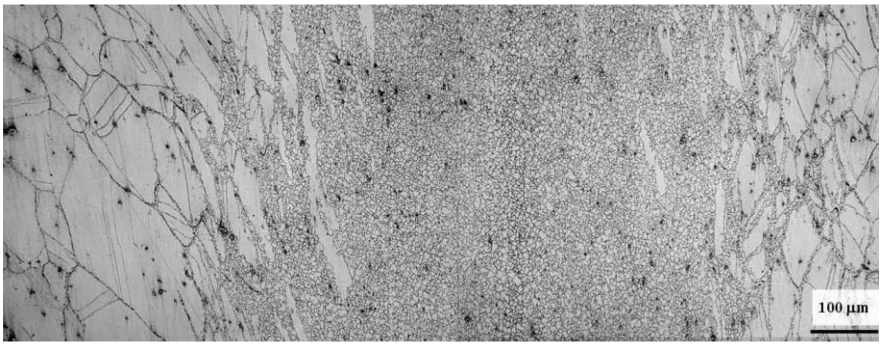

Figure 4: Microstructure of joining zone of alloy EI698VD.

The width of HAZ with decreased microhardness almost coincides with that of the heating zone above solvus temperature $T_{\gamma'}$ determined by calculations at different values of the FW process parameters, which is indicative of the adequacy of the mathematical model. Scanning electron microscopy (SEM) shows that the booth primary and secondary γ'-phase particles is dissolved within this softening zone during friction heating process (Fig. (5)).

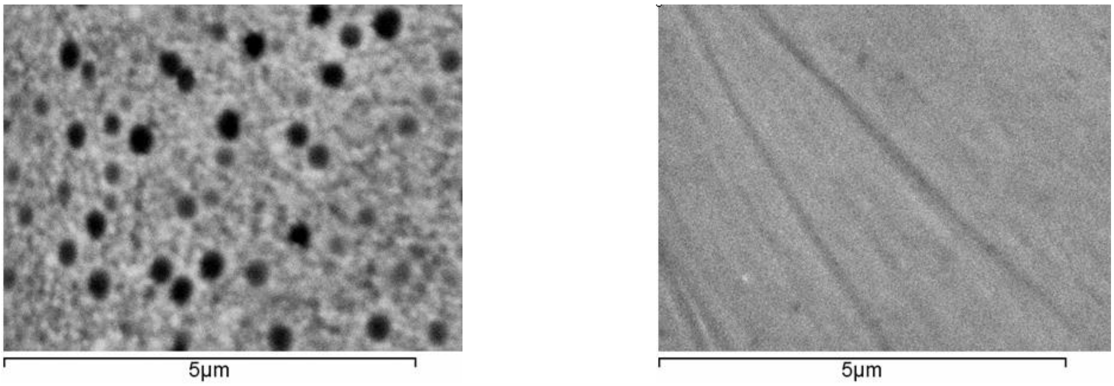

(a) (b)

Figure 5: SEM image of alloy EI696VD base metal (a) and joining zone metal (b).

4. CONCLUSIONS

Analysis of the calculation data obtained on the basis of the developed mathematical model of friction welding showed that the solidus temperature of alloy EI698VD is achieved within the contact zone. It is likely that the melt is formed in separate regions of the contact zone, which further on is subjected to intensive deformation, move in a radial direction, and is pressed out from the joint into a flash.

At any values of the FW process parameters, one might expect dissolution of the γ'-phase particles in the joining zone. To minimise width of the zone of phase transformations, it is necessary to use a comparatively low values of circumferential velocity, and high values of pressure.

5. ACKNOWLEDGEMENTS

The authors acknowledge CAPES, FAPEMIG and CNPq for their support, Postgraduate Program in Mechanical Engineering at the Federal University of Uberlandia and E.O. Paton Electric Welding Institute.

6. REFERENCES

Friction Welding. “Machine Building: Encyclopaedia”. V. III-4. – M.: Mashinostroyeniye, 2006.

Kuchuk-Yatsenko, S.I., Zyakhor, I.V. “Method of friction welding and machine for its application”. Pat. 546460 Ukraine, Int. Cl. V 23 K 20/12. Publ. 15.11.2004.

Zyakhor, I.V. “Modern equipment for friction welding”. *The Paton Welding Journal*, Vol.7, 2001, pp. 48-52.

7. RESPONSIBILITY NOTICE